47TH TURBOMACHINERY & 34TH PUMP SYMPOSIA
HOUSTON, TEXAS | SEPTEMBER 17-20, 2018
GEORGE R. BROWN CONVENTION CENTER

DESIGN AND VERIFICATION TESTING OF BALANCE PISTON FOR HIGH-VISCOSITY MULTIPHASE PUMPS

Ina Ekeberg
Senior Process Engineer, Technology Development
OneSubsea, a Schlumberger Company
Bergen, Norway

Halfdan Knudsen
Process Engineer, Fluid Dynamics
OneSubsea, a Schlumberger Company
Bergen, Norway

Rune Angeltveit
Mechanical Engineer, Fluid Dynamics
OneSubsea, a Schlumberger Company
Bergen, Norway

Hans Fredrik Kjellnes
Product Champion, Subsea Multiphase Boosting
OneSubsea, a Schlumberger Company
Bergen, Norway

Pierre-Jean Bibet
Expert in Pumping Systems
Total E&P
Paris, France

Knut Klepsvik
Senior Process Engineer, Fluid Dynamics
OneSubsea, a Schlumberger Company
Bergen, Norway

Erik Torbergsen
Section Manager, Technology Development
OneSubsea, a Schlumberger Company
Bergen, Norway

Ina Ekeberg is a Senior Engineer at OneSubsea Processing in Bergen, Norway. She joined OneSubsea in 2006 and has been involved in technology development and engineering of subsea processing systems, with special focus on multiphase pumps. She holds a M.Sc. degree from Delft University of Technology in 2005.

Pierre-Jean Bibet is Expert in Pumping Systems, Centrifugal Pumps and MPPs at Total E&P in Paris, France, who has been working in the Rotating Machinery Department of the Technology Division since 2003. His work concentrates on subsea boosting projects, following 23 years of professional experience with pumps, especially with Multiphase Pumps (MPP).

Halfdan Knudsen is a project engineer at OneSubsea Processing. He graduated from the Norwegian University of Science and Technology in 2013. During his time in OneSubsea, Halfdan has been involved in two major EPC projects. His work has been focused on multiphase pump performance and pump operation and protection.

Knut Klepsvik is a Senior Engineer at Onesubsea Processing in Bergen, Norway. He holds a M.Sc. degree from the Norwegian University of Science and Technology in 2005. His work covers engineering and technology development from several industries with focused knowledge in pumps and rotating machinery performance.

ABSTRACT

OneSubsea was awarded a project involving the development and testing of a HighBoost multiphase pump (MPP) for boosting unprocessed multiphase well streams with liquid viscosities up to 800 cP (0.8 Pa·s). The viscosity requirement surpasses the existing viscosity range of dynamic multiphase pumps and the difference in viscosity for the liquid and gaseous phases is larger than in any other comparable test programs. Results from the full-scale testing have shown remarkable balance piston flow mechanisms affecting both rotordynamic behavior and step-changes in volumetric efficiency for the pump assembly. These phenomena have been studied in detail during the extensive testing, and further investigated with corresponding analysis. The work described in this paper has resulted in a design improvement and a solution for this demanding subsea boosting application. Furthermore, the

analysis also shows that more research is needed to fully understand high viscosity multiphase flow in seals and balance pistons. The comprehensive technology development work was conducted within the EPC project timeframe and has realized the operator's requirements of boosting the subsea production of a demanding oil-field.

CONTEXT OF THIS WORK

By Bernard Quoix, Total E&P, Senior Fellow and Head of Rotating Machinery Department

This paper must be viewed in the context of a world first realization of a Subsea Multiphase Pumping application to produce high viscous oils. Some of the world's largest reserves are heavy oil reservoirs, defined as liquid petroleum of less than 20°API gravity or more than 200 cP (0.2 Pa·s) at reservoir conditions, which with increasing water cut, can lead to very high emulsion viscosities to be pumped.

In 2013, the authors' companies initiated an Engineering, Procurement and Construction (EPC) project to design and build a subsea pump system including pumps capable of boosting oil and gas with liquid viscosity up to 800 cP (0.8 Pa·s). The pump manufacturer selected two 4,700 hp (3.5 MW) HighBoost Multiphase Pumps with a maximum differential pressure (dP) of 1,595 psi (110 bar). The high power rating was set in order to meet the operational requirements at high viscosity and was to be the most powerful multiphase pump ever installed subsea. The balance piston was designed to handle the high viscosity. In addition to the standard volumetric losses versus viscous losses balancing, heat generation was also considered.

Figure 1 View of the HighBoost MPP station

During a wide performance mapping full-scale pump test, the project team discovered a phenomenon creating a major step change in balance piston through-flow along with significant rotor vibrations. The phenomenon manifested itself as transitional, occurring only at intermediate viscosities, intermediate gas volume fractions (GVF), and intermediate differential pressures.

Boosting a high-viscous multiphase flow with a HighBoost pump introduces new challenges, and requires the development of a new expertise to handle multiphase pumping in very laminar flow regimes. Although several pump components were subject to new design criteria, this paper focuses on the balance piston, which proved to play a vital role in this operational range extension.

The successful execution of this project is the result of joint efforts and close collaboration among all team members. The pump system was successfully installed, commissioned and started during the spring of 2017 to boost the viscous production. It has been running with 100% availability following the startup.

INTRODUCTION

Subsea Boosting

Applying pumps on the seabed to boost the production of oil and gas has been a valuable artificial lift method for 25 years. Both twin screw pumps and dynamic pumps have been utilized for the purpose, but dynamic pumping is the only technology in operation today. Currently installed subsea boosting pumps are located at water depths up to 10,000 ft (3,000 m), with up to 21 miles (34 km) tieback distance to topside host facilities with power supply and pump control system. Prior to the range-extension described in this paper, existing subsea multiphase boosting pumps had been qualified up to 2,900 psi (200 bar) differential pressure, 8,800 gpm (2,000 Am3/h) pump flowrate, 200 cP (0.2 Pa·s) liquid viscosity, 5,100 hp (3.8 MW) shaft power, and GVF from 0-1.0.

Pump

The pump type applied in the current work is a dynamic multiphase pump with open helicoaxial impeller and diffuser stages (Figure 2). A subsea pump is vertically aligned, arranged with a pump at the bottom and a variable speed controlled, oil-filled, electrical motor on top. A multiphase pump can be arranged with up to 13 helicoaxial stages, typically with one to three different designs to account for process fluid compression. The helicoaxial stages are designed to balance Coriolis and centrifugal forces in order to generate high head while avoiding gas lock effects. Hydrodynamic tilt pad thrust bearings are applied to handle the down thrust generated by the impellers. For HighBoost pumps, i.e., pumps with differential pressures above 725 psi (50 bar), a balance piston is included to reduce the load on the thrust bearing (Figure 3). The shaft is radially supported by tilt pad journal bearings at pump drive end (DE) and nondrive end (NDE). Pump and motor shafts are connected with a flexible coupling. Motor and bearings are lubricated by over-pressurized barrier fluid, securing a clean environment for motor and bearings. Mechanical seals, which are separating the process from the barrier fluid, allow a modest leak of barrier fluid into the process. A subsea MPP is placed in a subsea pump station with valves, gas-liquid mixing unit, and recirculation line.

Process media

One of the main challenges with designing subsea boosting pumps is the varying process conditions entering the pump. A subsea boosting pump is typically a life of field installation, meaning that it must boost new and healthy wells, increasing water cut and emulsions, GVF variations, as well as solids production. The boosting pumps need to be highly flexible in terms of operating conditions, and utterly robust.

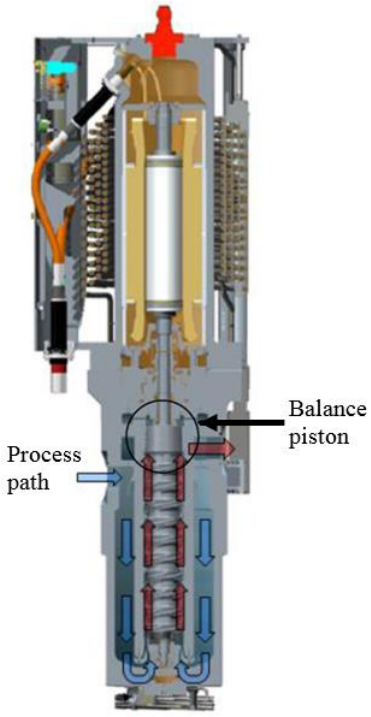

Figure 2 High Boost Multiphase Pump

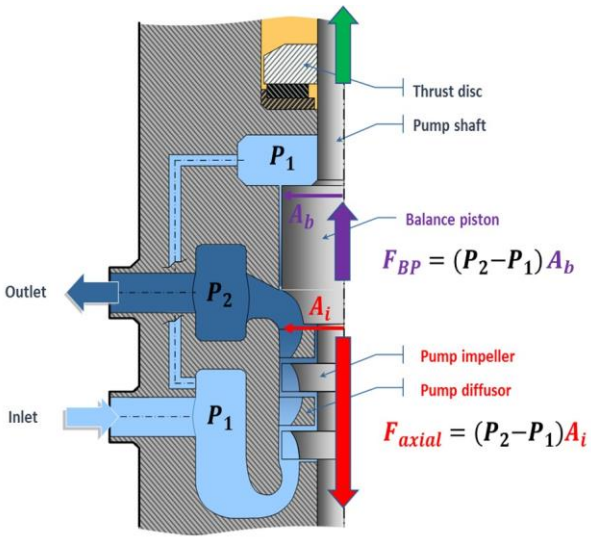

Figure 3 High Boost Multiphase Pump Balance Piston Principle

In the currently described project, the liquid viscosity of 800 cP (0.8 Pa·s) was significantly higher than previous experience. Pumping of high viscosity fluids with a dynamic pump has to a small degree been explored in the past. New challenges were awaiting, and the balance piston demonstrated its key role in this rotordynamic system.

PRIOR ART MPP BALANCE PISTON

Prior art MPP balance piston was developed by the authors' companies and JIP partners in a technology development program, and is described by Bibet et al. (2013). The outcome of the program was an MPP capable of supplying 2,175 psi (150 bar) differential pressure at GVFs up to 0.6 and viscosities up to 30 cP (0.03 Pa·s). A geometrically complex multisegment balance piston (Figure 4) was required to control the challenging operating conditions.

The radius of the balance piston rotating component R_i is set by the thrust balancing requirements. Design criteria for the seal length L and gap clearance C_r are limiting volumetric losses, avoiding excessive temperatures, and minimizing unwanted impact on rotordynamic stability. The balance piston inlet swirl is reduced by means of swirl brakes. In multisegment balance pistons, additional swirl brakes are included at the start of each segment.

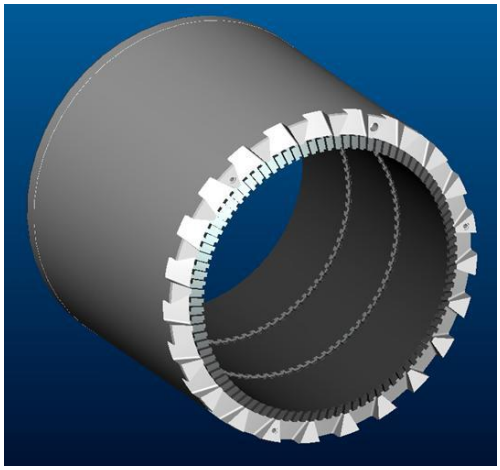

Figure 4 MPP Balance Piston Liner in Three Segments with Swirl Brakes

PREDICTING HIGH VISCOSITY MULTIPHASE BALANCE PISTON PERFORMANCE

For high energy pumps with balance piston seals, detailed knowledge about the flow pattern and corresponding rotordynamic interaction is essential, as it might control the overall dynamics of the pump. In the design of subsea boosting pumps for high-viscosity well stream, existing models and prior research on annular seals have limitations. Most research efforts on annular pressure seals focus on predicting the behavior of single phase fluid at turbulent conditions. Annular seals in multiphase pumps may be subject to GVFs between 0 and 1.0, and boosting of heavy oil wells may yield liquid viscosities of several hundred centipoise. The balance piston is

the dominating annular seal in a HighBoost MPP. It has axial flow driven by the full differential pressure range of the pump, and its design greatly impacts both pump efficiency and rotordynamics.

General annular seal flow

Axial Reynolds number Re_{ax}, tangential Reynolds number Re_{tan} and Taylor number Ta are normally used when analyzing annular seals with axial flow (illustrated in Figure 5). Reynolds numbers are calculated from:

$$Re_{ax} = \frac{\rho C_r u_{ax}}{\mu}$$

and

$$Re_{tan} = \frac{\rho C_r \omega R_i}{\mu}$$

where ρ and μ are respectively the density and dynamic viscosity of the fluid, u_{ax} the axial velocity of the throughflow and ω the rotational velocity of the inner cylinder. Reynolds numbers are applied to predict transition between laminar and turbulent flow to, for example, select adequate friction coefficients. Furthermore, the Rossby number Ro, can be described by the ratio axial to tangential Reynolds numbers:

$$Ro = \frac{Re_{ax}}{Re_{tan}} = \frac{u_{ax}}{\omega R_i}$$

A Rossby number below unity indicates that centrifugal forces dominate over inertial forces. The Rossby number is of particular interest in multiphase flow, where phase separation is a function of the force ratio.

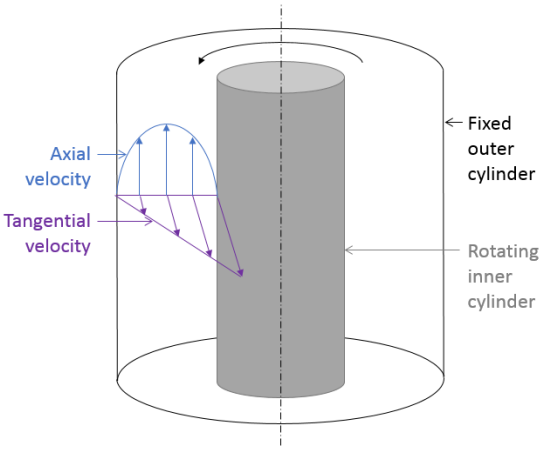

Figure 5 Schematic view of annular pressure seal velocity profiles

The Taylor number describes the ratio of inertial to viscous forces and it is used to predict the onset of flow regimes, including various forms of Taylor vortex flow (e.g. Yamada [1962] and Werely & Lueptow [1999]). The onset of Taylor vortex flow is delayed when an axial flow component is present. Taylor number is calculated from

$$Ta = \frac{\rho^2 C_r^3 \omega^2 R_i}{\mu^2}$$

Common for the analytical approaches to annular seal flow is the description of one fluid. To allow for this approach, it is necessary to describe the two-phase fluid in terms of mixture properties.

Mixture properties

When defining mixture properties, the most common approach is to assume a homogeneous flow, where gas and liquid travel with the same velocities, i.e., no slip conditions. In reality, two-phase flow is quite complex and this assumption is not necessarily correct. Assuming a homogeneous mixture, the mixture density ρ_m can be described by:

$$\rho_m = GVF\rho_g + (1 - GVF)\rho_l$$

where ρ_g and ρ_l are densities of the constituents. Published models for gas-liquid mixture viscosities deviate greatly, leading to orders-of-magnitude differences in calculated Reynolds numbers. McAdams et al. (1942) conducted experiments on vaporization inside horizontal tubes and compared their results with a mixture viscosity model using weighted reciprocal viscosity. Cicchitti et al. (1960) found a very different mixture viscosity fitting their experiments on steam and water. Dukler et al. (1964) evaluated test data from several scientists and applied single-phase and two-phase data in several experimental setups to evaluate friction loss models. Their proposed model, which predicts a mixture viscosity based on phase volume fraction and kinematic viscosities, is applied in numerous industrial applications. Beatty and Whalley (1981) found that the mixture viscosity increases above the liquid viscosity in a region up to GVF 0.6 and continuous with a relatively high mixture viscosity (higher than what Dukler et al. (1964) predicted) until it reaches pure gas. Lin et al. (1991) found two-phase viscosity effects originating from different velocities of the phases. Their model applies an empirical exponent based on data from tubing experiments. Arauz & San Andrés (1998) describe a mixture viscosity model with a discontinuity at GVF 0.3. The model is similar to Beattie and Whalley (1981) up to GVF 0.3 with effective viscosity larger than liquid viscosity. At GVF 0.3, the mixture viscosity model makes a step change towards a viscosity resembling gas viscosity.

In Figure 6 the various mixture viscosity correlations are plotted as two-phase multiplier versus GVF. In this figure μ_l/μ_g =1000, pressure = 1,015 psi (70 bar) and gas properties of nitrogen are used. The two-phase multiplier Φ is defined as:

$$\Phi = \frac{\mu_m}{\mu_l}$$

Applying mixture viscosity correlations is hence a high gamble, unless experimentally validated for relevant geometries and

conditions.

Table 1 Mixture Viscosity Correlations

Author	Mixture viscosity correlation
McAdams et al. (1942)	$\mu_m = \left(\frac{x}{\mu_g} + \frac{1-x}{\mu_l} \right)^{-1}$
Cicchitti et al. (1960)	$\mu_m = x\mu_g + (1-x)\mu_l$
Dukler et al. (1964)	$\mu_m = \rho_m \left[x\left(\frac{\mu_g}{\rho_g}\right) + (1-x)\left(\frac{\mu_l}{\rho_l}\right) \right]$
Beattie and Whalley (1981)	$\mu_m = \mu_l(1-GVF)(1+2.5GVF) + \mu_g GVF$
Lin et al. (1991)	$\mu_m = \frac{\mu_l \mu_g}{\left[\mu_g + x^{1.4}(\mu_l - \mu_g)\right]}$
Arauz & SanAndrés (1998)	$GVF \le 0.3$: $\mu_m = \mu_l + 2.5 \left(\frac{\frac{\mu_g}{\mu_l} + 0.4}{\frac{\mu_g}{\mu_l} + 1} \right) GVF$ $GVF > 0.3$: $\mu_m = \left\{ \left[\left(\frac{\lambda_+}{\mu_g} - \frac{1}{\mu_+} \right) + \left(\frac{1}{\mu_+} - \frac{1}{\mu_g} \right) \lambda \right] \frac{1}{(\lambda_+) - 1} \right\}^{-1}$ *where* $\lambda_+ = \frac{0.3}{0.3 + 0.7\frac{\rho_l}{\rho_g}}, \mu_+ = \frac{1.3\mu_l^2 + 1.75\mu_l\mu_g}{\mu_l + \mu_g}$

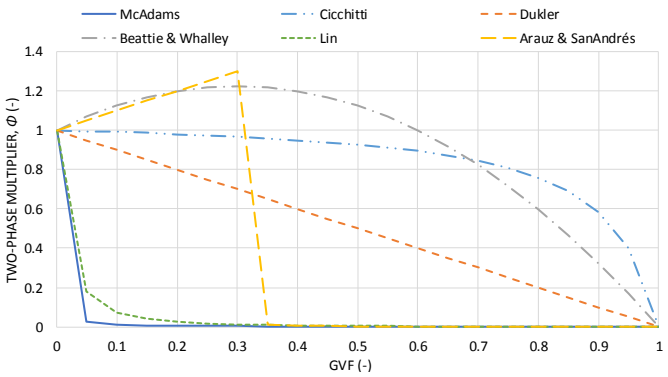

Figure 6 Two-Phase Multiplier defined by various Mixture Viscosity Correlations (Table 1)

Two-phase flow effects

The mixture viscosity correlations in prior art is mainly developed for pipe or tube flow. The multiphase flow pattern experienced in pipe flows has far less gradients than flow fields within a balance piston clearance. Two-phase flows exposed to centrifugal forces in annular seals yields further complexity to the flow field. The large centrifugal forces have separating effects on the two-phase flow. The result of complete separation will be a liquid film along the static outer diameter and a gas film along the rotating inner cylinder. This can be referenced to basic annular flow effects where liquid film on static surface can alter the effective surface friction coefficients. Further, the liquid film can adapt 2D waves and ultimately wave heights can block the clearance gap. 2D waves may then generate variations in shaft torque, droplet entrainment rates, and velocity gradients. Beatty and Hughes (1990) developed a mathematical model of the leak rate behavior in turbulent stratified cryogenic two-phase seals. They found that the modelled leak rates are very similar for stratified and homogeneous flow and suggest that leak rates can be calculated without precise information about the actual flow pattern or interfacial shear stresses.

Presence of Taylor vortices may also impact the homogeneity of the two-phase mixture and the dynamic forces. Shiomi et al. (1992) experimentally studied Taylor vortex flow with gas bubbles and published photographs of rings of gas bubbles formed at the inner cylinder. A criterion for generating Taylor-vortex is to have significant tangential velocities relative to the axial velocities, often presented as a Rossby number lower than 0.2. The balance piston operation is in most cases in the range of higher Rossby numbers, hence the Taylor-vortex is assumed not to be significant.

Rotordynamic properties

Rotordynamic properties of annular seal flow have been studied for many decades. Investigated fluids are typically nitrogen or a low-viscosity liquid like water (or light oils), and bulk flow models have been developed that enable efficient prediction of seal dynamic characteristics (Black & Jenssen [1970], Childs [1983]). Only a few experiments with higher viscosities have been published, reflecting the exceptionality of such applications. Childs et al. (2006) summarize research on high viscosity and laminar flow. A few research articles have been published on multiphase flow in annular seals. Iwatsubo & Nishino (1994) conducted experiments on static and dynamic characteristics of an annular seal with two-phase flow. They reported that, generally, fluid forces reduce with increasing GVF, resulting in reduced stabilizing seal effects at multiphase conditions. In addition, at high GVF, the measured forces fluctuated greatly. San Andrés (2012) further developed a bulk flow model for two-phase flow in which the Reynolds numbers are modified with a mixture viscosity presumed to describe the two-phase mixture. In the continuation of his research, San Andrés et al. (2016) and Tran (2018) conducted experiments to validate the previously developed model but encountered surprising dynamic stiffness results, possibly due to nonhomogeneity of the mixture. More analytical and experimental research is published on annular seal wet gas flow (i.e., Vannini et al. [2011]); however experimental data on 0<GVF<0.9 is limited.

In-house experience

The manufacturer of the current pump has studied and developed models for annular seal flow for use in multiphase pumps, liquid pumps and wet gas compressors. Storteig (1999) developed models for single phase balance pistons. Bibet et al. (2013) described the development of multiphase balance pistons. The dynamic response of the multiphase balance piston is found from inhouse proprietary methods, including CFD

simulation with different whirl perturbation methods. The experimental experience comes from testing full-scale multistage pumps with balance pistons. The two-phase effects described above are accounted for in the multiphase CFD model, by extensive test data calibration. Therefore, the variation in density, gas fraction, temperature, and viscosity within the seal clearance is included in the fluid dynamic and rotor dynamic performance analysis for the balance piston design.

Limited experience on high-viscosity multiphase balance pistons set requirements for extensive testing on current application. The test results are vital to verify the performance of the product and to serve as input to extended design and prediction models.

TEST SETUP

Pump

The experimental setup includes a 5,000 psi (345 bar) design pressure pump, built for subsea deployment. The pump has a 4,700 hp (3.5 MW) motor with running speeds from 1,500 rpm to 4,600 rpm. It is a HighBoost multiphase pump with 11 helicoaxial impeller and diffusor stages and a balance piston. The balance piston is located downstream of the impeller and diffusor stages, at the DE of the pump shaft. It is connected to the pump outlet pressure on the lower side and the pump inlet pressure at the top (Figure 2 and Figure 3). Despite considerable leak rates at low viscosity, the initial balance piston was a short seal with L/D = 0.2 and inlet swirl brakes. This design was selected to enhance stiffness contribution and avoid excessive temperatures at high viscosity operation. To map the performance of the balance piston, the internal balance piston return channels were plugged and the flow was routed out of the pump, as shown in Figure 7. The balance piston leak rate Q_{leak} was measured by means of multiphase flow meter (MPFM), which in addition logged GVF, pressures, and temperatures.

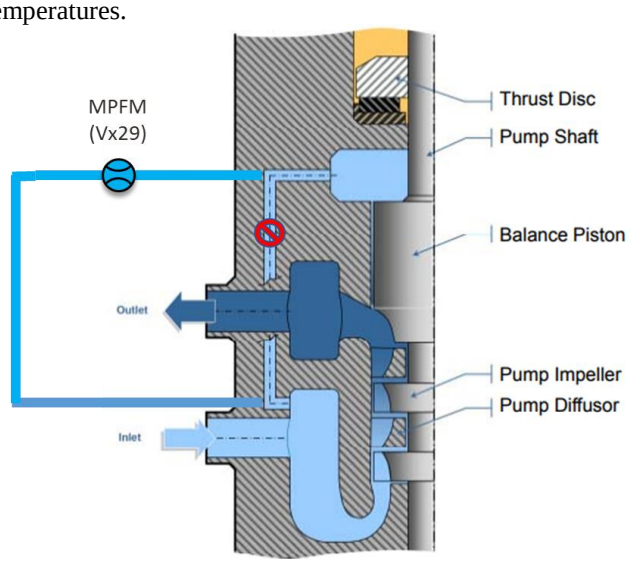

Figure 7 External balance piston return line

The test was conducted at pump inlet pressures (hence balance piston outlet pressures) between 145 and 508 psi (10 and 35 bar) with differential pressures up to 1,595 psi (110 bar), yielding a generous span in axial velocities and compression ratios. By means of a variable speed drive, the full speed range of the pump was utilized, enabling an extensive range of tangential velocities. The pump was equipped with shaft proximity probes and casing velocity probes for vibration measurements. There were two orthogonally positioned proximity probes at three axial locations: pump NDE, pump DE and motor NDE, as illustrated in Figure 8.

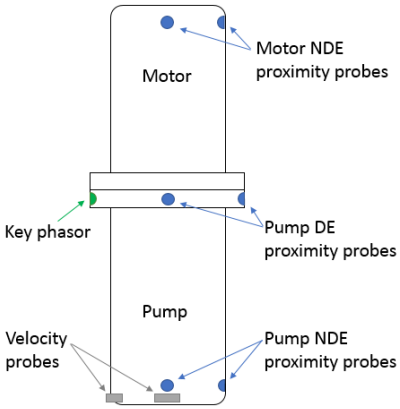

Figure 8 Pump Vibration Monitoring Set-Up

Flow Loop

A high viscosity multiphase flow loop was designed and built prior to the full-scale testing of the pump. A principle sketch of the flow loop is shown in Figure 9. Two separate single-phase lines leave the 1,413 ft^3 (40 m^3) two-phase separator. Between the separator and the mixing point the liquid is cooled by two process coolers mounted in parallel. Both gas and liquid flowrates are measured separately before the mixing point. For gas measurements, V-cone flow meters are used. Liquid flowrate is measured with an MPFM positioned on the liquid metering section. Any gas carry-under in the liquid line will be identified by the MPFM. Flowrates are individually regulated by control valves on the liquid and gas lines. The pump discharge pressure is regulated with remotely operated choke valves downstream the pump.

A cooling circuit provides fluid to the process coolers located on the liquid line. Suction temperature control is achieved by flow control valves on the cooling circuit and variable speed drives on the cooling circuit circulation pumps.
The flow loop accommodated all required test conditions given in Table 2.

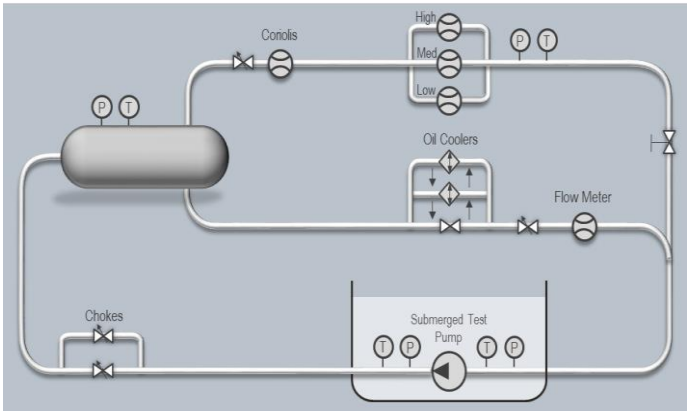

Figure 9 High Viscosity Flow Loop

Table 2 Pump Design Conditions and Test Conditions

	Design conditions	Test conditions		
Flow rate	>650	440-940	Am3/h	At pump inlet
GVF	0.10-0.68	0-0.75	-	At pump inlet
Liquid viscosity	1-833	1-800	cP	Continous operation
Liquid viscosity	1 300	30 000	cP	Start-up conditions
Suction pressure	15-43	10-35	bara	
Differential pressure	>98	10-110	bar	
Speed	1500-4600	1500-4600	rpm	

Fluids

To achieve the desired range of liquid viscosities, three different liquids were applied:

- Fresh water
- Hydraulic oil with viscosity grade 180
- Gear oil with viscosity grade 800

The liquid viscosity was further adjusted by regulating the liquid temperature in the flow loop. Figure 10 illustrates that oil viscosities from 50 to 800 cP (0.05-0.8 Pa·s) could be obtained with the manageable temperature range (104-176 °F [40-80 °C]). During start-up of the pump, the liquid temperature would be significantly lower. At 39 °F (4 °C), the high-viscosity oil had a viscosity of 30,000 cP (30 Pa·s). The gas phase was nitrogen, which was added to the mixture in quantities ranging from 0 to 0.75 GVF.

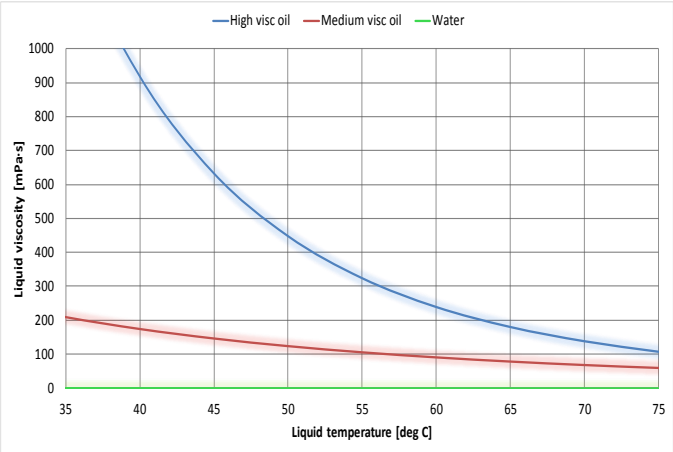

Figure 10 Viscosity profiles

TEST OBSERVATIONS AND DISCUSSIONS

Pump Performance Testing

The pump performance test campaign started with water and nitrogen as process media. The results were matching the predictions well. Viscosity testing started with what was assumed to be the worst case: operation at 800 cP with varying magnitudes of nitrogen, and startup with cold oil in the range of 30,000 cP. Again, the pump performed exceptionally in terms of hydraulic performance and rotordynamic performance and the viscous head degradation was significantly less than the predictions.

The tests were performed in a typical pump performance test manner: constant speed curves from *high flow & low dP* to *low flow & high dP* (Figure 11). Under these conditions the balance piston conditions start at *low dP & low* Q_{leak} and continue towards *high dP & high* Q_{leak} (Figure 14). The flowrate was changed by operating a choke downstream of the pump.

When testing at viscosities between the extremes, unforeseen behaviour was observed: abrupt high asynchronous vibrations occurred within the pump operating envelope. In some cases, the amplitude exceeded a defined trip limit set to protect the pump. Figure 11 shows typical examples of such speed curves, where conditions with high asynchronous vibrations are highlighted.

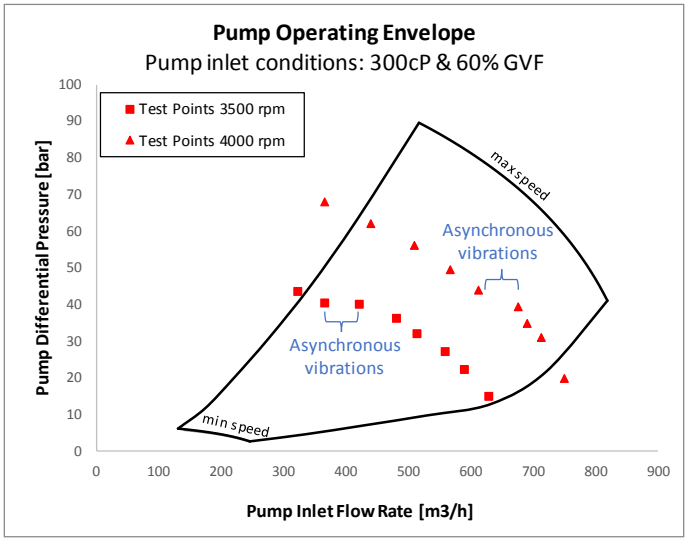

Figure 11 Pump performance map – asynchronous vibrations detected

Figure 12 and Figure 13 are waterfall plots from the NDE proximity probes during the asynchronous vibration onset for the two speed curves. The synchronous vibration can be seen as distinct steady peaks at 66.7 Hz (4,000 rpm) and 58.3 Hz (3,500 rpm), respectively. Such vibration is always present in rotating machinery, but as long as sufficient damping is provided, it does not pose any risk of harmful operation.

Transient asynchronous vibration peaks can be seen at other frequencies. These are mainly super-synchronous, with forward precession. The super-synchronous vibrations did not appear at a fixed frequency, but varied between 66-91 Hz or 1.07-1.44 times the rotational frequency depending on temperature, GVF and pressures. In Figure 12 and Figure 13, the asynchronous frequency is moving slightly due to change in temperature. At lower GVF, the transient vibrations occurred at sub-synchronous frequencies. In these cases, the dominating vibration frequency could shift between forward and backward precession.

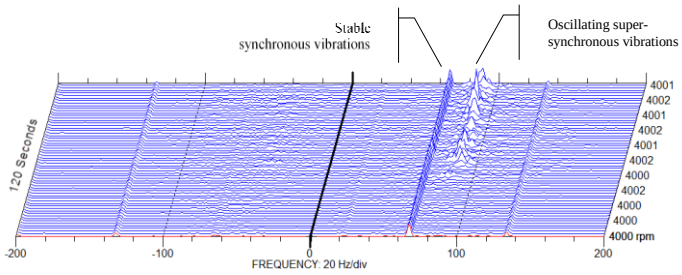

Figure 12 Waterfall plot from 4,000 rpm (66.7 Hz) in Figure 11. Test point #4 from right

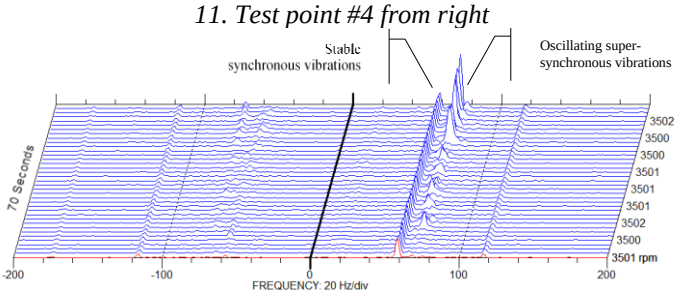

Figure 13 *Waterfall plot from 3,500 rpm (58,3 Hz) in Figure 11. Test point #6 from right*

The facts that the vibrations were occurring abruptly, and that the precession could shift, indicate that the vibrations are self-excited. The continuously changing process conditions which affect dynamic forces in impellers, balance piston, and seals explain the changing frequency of the triggered mode. As previously described, the vibration probes measure shaft deflection at two axial locations of the pump shaft. Although this set-up is not sufficient to describe the complete mode shape, the phase angles and deflection amplitudes indicate a first order bending mode with higher amplitudes at NDE. This mode shape is supported by rotordynamic sensitivity analyses, where the balance piston dynamic coefficients are altered.

Balance piston

The pump performance testing revealed that adjusted balance piston conditions significantly impacted the pump rotordynamic behaviour: restricting the balance piston leak rate with a choke valve downstream of the balance piston, would change the onset of asynchronous vibrations. (It was verified that the increased load on the thrust bearing did not affect the results.) The further experiments were, therefore, mainly focused on the balance piston.

In Figure 14, the measured mass flowrate across the balance piston is plotted against pump differential pressure for the two speed curves from Figure 11. A significant step-change in leak rate can be seen at the instance the vibrations occur. This occurrence will be referred to as the *transition*. Studying the pump performance curves from Figure 11 in detail, the increased balance piston leakage can also here be seen as a horizontal shift in the constant speed curves. The two speed curves in Figure 14 coincide, indicating that a rotational speed variation of 15% have minimal impact on the leak rate and transition. The fluid conditions were set for pump suction conditions, and are therefore, not identical for the balance piston conditions. Figure 15 demonstrates the variations in average liquid viscosity and GVF.

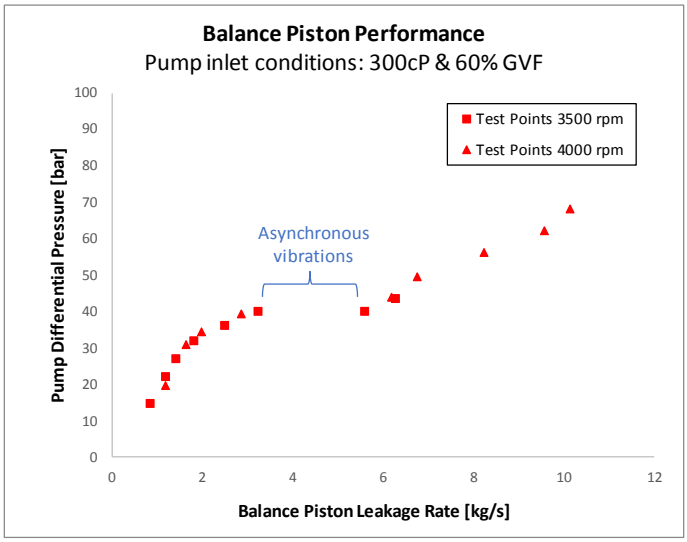

Figure 14 Balance piston leak rate

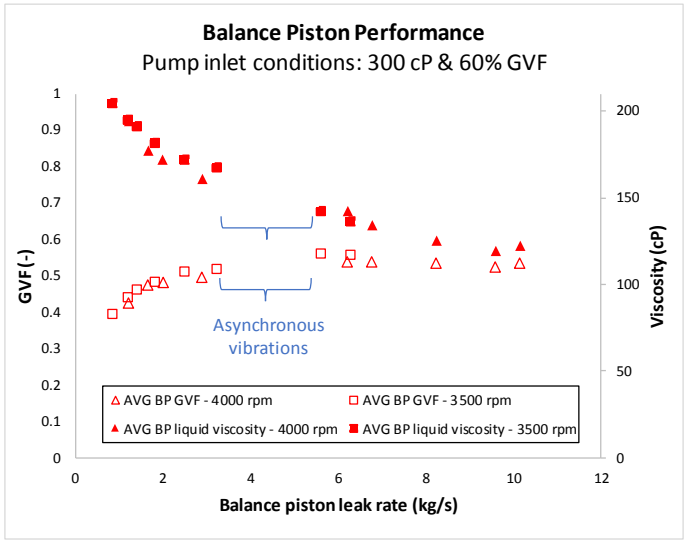

Figure 15 Average balance piston GVF and liquid viscosity for test points in Figure 14

The transition occurred at certain combinations of dP, μ_l and GVF. In Figure 16, pump dP and μ_l and GVF at pump outlet (balance piston inlet) conditions are shown. The circles mark the test points logged, and the surface body in the same plot, illustrates the transition threshold. The vibrations occurred at intermediate differential pressure, which varied with viscosity and GVF. Stable operation was achieved at any side of the transition.

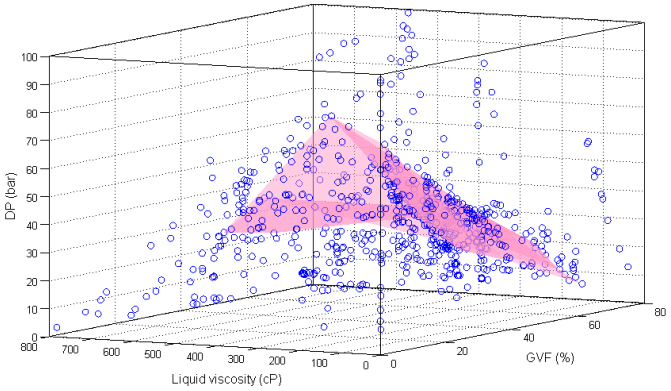

Figure 16 Pump dP, liquid viscosity and GVF at pump outlet. Circles are test points. Surface body is transition threshold.

Evaluations and analyses were performed to find out what caused the abrupt change in leak rate and dynamic forces. Some key conclusions are:

- Due to unidentified effective viscosities discussed earlier in this paper, Reynolds numbers could not be used to examine the transition.
- In Figure 17, calculated Rossby numbers for the test points are shown. Test points where transition was detected are shown in the upper part of the figure. The figure demonstrates that centrifugal forces dominate over inertial forces, i.e. $Ro < 1$, for the majority of the test points. It can also be seen that the transition was detected at an intermediate range of Rossby numbers, but not all test points in this range demonstrated transitional behavior.
- When evaluating annular seal flow, torque measurements are typically used to detect changes in friction factors. As the balance piston represents only a minor portion of the pump torque, potential variance in balance piston torque could not be detected in this setup.
- The fact that the transition occurred at different pump absolute and relative flowrates proves that impeller off design operation or undesired flow patterns upstream the balance piston did not affect the inception.
- Bubble sizes and flow regimes are not measured. However, upstream the balance piston the flow is mixed through 11 helicoaxial impeller stages.

The test setup had limited instrumentation measuring balance piston dynamics. Hence, it is difficult to determine the exact physical phenomenon occurring during the transition. To further investigate the root cause, numerical studies were initiated.

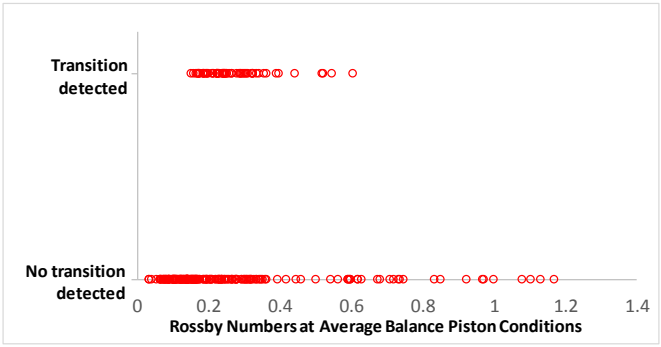

Figure 17 Rossby numbers

DYNAMIC SIMULATIONS

To further investigate the flow pattern in multiphase viscous fluids, numerical studies were done of specific test conditions. A multiphase CFD approach was used to both study fluid phase interaction and the integrated forces acting on the shaft surface. The CFD model includes an inlet cavity with part of the main flow upstream the balance piston, as can be seen in Figure 18. Outlet cavity is set up with an opening boundary condition to enhance numerical stability. A mesh size of 350,000 nodes was found as a minimum to capture the flow patterns by comparing single phase results with conventional seal design tools.

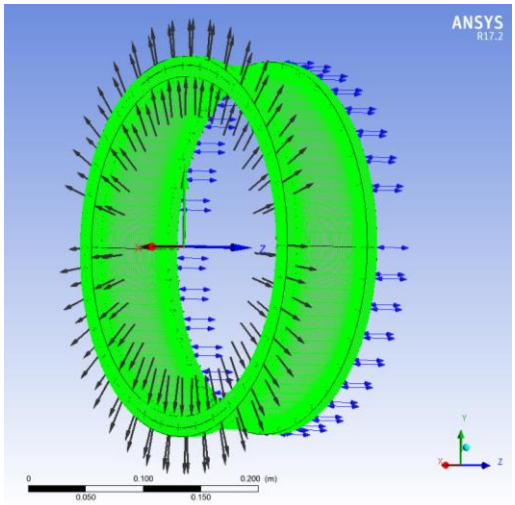

Figure 18 Balance piston CFD model setup

By running sensitivity on dP across the balance piston it was intended to see the effect of varying Rossby numbers for the flow field. Test data at 4000 rpm rotational speed, 0.6 GVF and 300 cP (0.3 Pa·s) at pump inlet were input to in the simulations. At low dP, the tangential forces are clearly found to be dominating and resulting in phase separation within the balance piston clearance. The gas is occupying the space proximal to the rotating surface and leaving the liquid phase with less

tangential velocity. Integrating the pressure to get the force acting on the rotating surface, shows that the cross coupled stiffness is almost negligible. The balance piston shows neutral rotordynamic coefficients.

At moderate dP, corresponding to test conditions with transition, there is a clear change in flow pattern. The local average GVF at balance piston inlet is now reduced to 0.4 due to compression of gas through the impeller stack and the local liquid viscosity is close to 200 cP (0.2 Pa·s). The average axial velocities are increasing as expected. But for certain sectors, there are high-velocity flow fields stretching from inlet to outlet and occupied of almost pure gas, as indicated in Figure 19 and Figure 20. Between the high-velocity sectors in Figure 20, there is found high liquid hold-up with low axial velocity. Corresponding static pressure across rotating surface is shown in Figure 21. The circumferential pressure is now uneven and dominated by the sectors of high velocity and corresponding low static pressure. The integration of rotating surface pressure is showing an oscillating direct stiffness with a negative average value. Oscillating cross coupled stiffness is present, but average values are lower than estimates with mixture viscosity models.

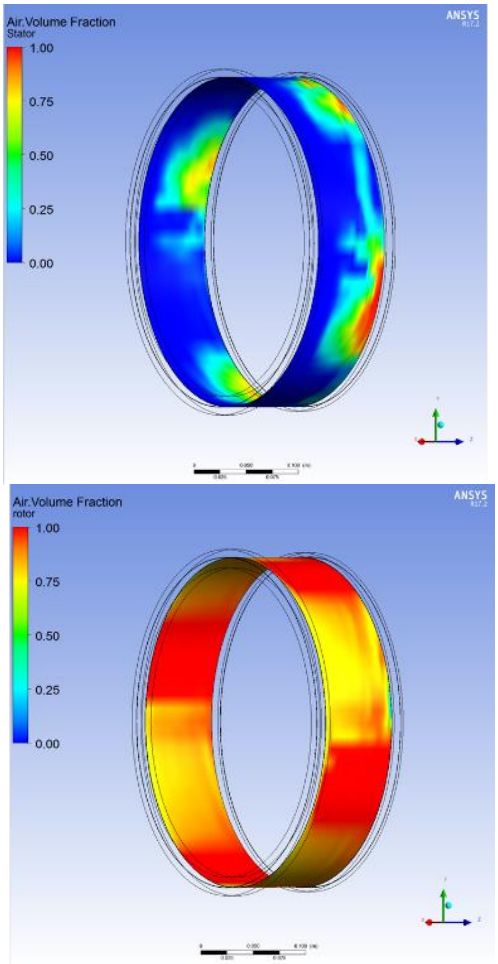

Figure 19 Balance piston CFD results. GVF on static (upper) and rotating (lower) surface for medium dP

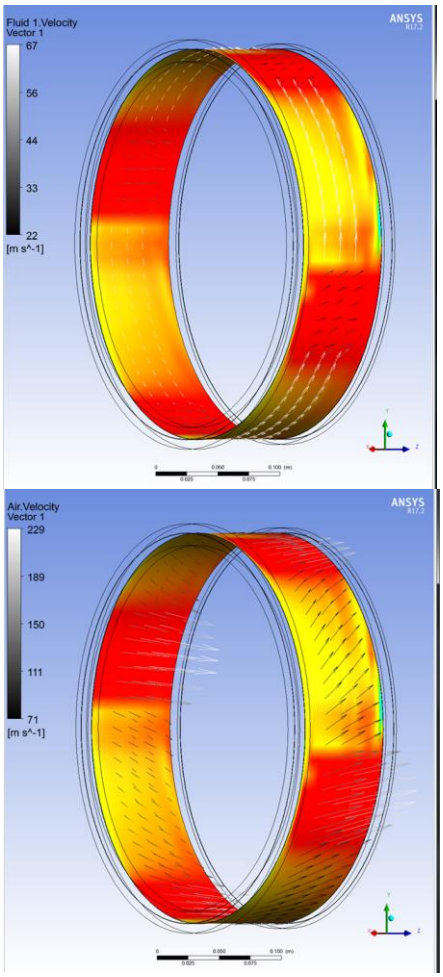

Figure 20 Balance piston CFD results. Liquid velocity (upper) and gas velocity (lower) vectors proximal the rotating surface for medium dP (surface colors identical to Figure 19)

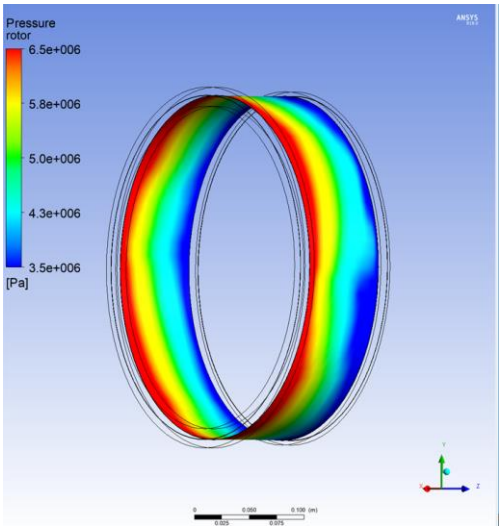

Figure 21 Balance piston CFD results. Static pressure on rotating surface for medium dP

At high dP across the balance piston, the flow field is showing more fluid phase interaction and mixing. Sectors of high gas velocities are more suppressed compared to moderate dP. The stabilizing Lomakin effect can be found, and hence, positive direct stiffness is calculated. The direct stiffness K_{xx} and cross-coupled stiffness K_{xy} for each simulated dP is shown in Figure 22. Values are normalized for the maximum direct stiffness calculated for operation on maximum differential pressure. The figure indicates a change in direction for the direct stiffness at medium differential pressure.

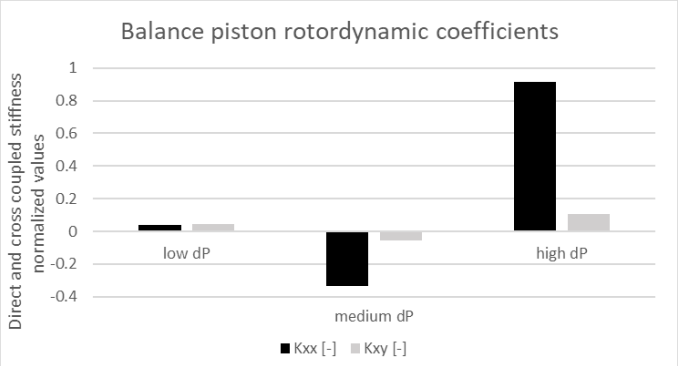

Figure 22 Balance piston rotordynamic coefficients from CFD simulations (average values)

The study continued with a sensitivity study on balance piston direct and cross-coupled stiffness in the rotordynamic model. The range of balance piston forces found from CFD strongly affects the systems first bending mode. The results show that damping factors for several modes decrease, compared with the initial Liquid Annular Seal (LAS) dynamic coefficients calculated with homogeneous fluid properties. The natural frequencies are also shifted and some modes correspond with frequencies observed during testing. The total damping, however, seems to be overestimated. The results indicate that negative balance piston stiffness can be a source to destabilize one or more of the rotor's natural frequencies.

A shift in stiffness was also observed by Tran (2018), in his experiments on rotordynamic forces on an annular pressure seal with GVF<0.1 and GVF>0.9. He found a significant drop in direct stiffness when the differential pressure was increased. Tran discussed that a possible cause of the stiffness drop might be an increase in friction factor at transitional Reynolds numbers, which would result in a reverse Lomakin effect. Interestingly, he also found that the stiffness drop occurs at lower differential pressures when the inlet preswirl is increased. The results might hence be related to the ratio axial to tangential velocities (Rossby number) or rapid increase in shear forces at seal inlet.

HIGH-VISCOSITY MPP BALANCE PISTON

New balance piston design

The pump was specified to operate at an extensive range of process conditions, and ensuring that the balance piston did not experience transitional regimes at any pump operating conditions was not practical. Therefore, a new balance piston designed to mitigate impact of flow transition was developed. In the new design, the clearance profile was changed to optimize velocities throughout the seal length.

In addition to valuable output from CFD simulations, fundamental principles for reducing Bernoulli effects were applied as design input. Lomakin effects are negligible at laminar conditions, but yield restoring effects at other operating conditions and was therefore part of the design criteria.

Testing new balance piston

The initial test matrix was repeated with the new balance piston installed. Pump performance was, as predicted, slightly improved due to reduced balance piston leak rate. Balance piston leak rates were studied along with shaft vibration measurements to evaluate how the design change affected the performance. As can be seen in Figure 23 and Figure 24, both the balance piston leak rate profile and vibration levels were significantly improved. Vague signs of transition could be noticed at certain conditions, but the new balance piston successfully mitigated unwanted shaft vibrations. The test matrix was completed without any vibration exceeding the maximum target level.

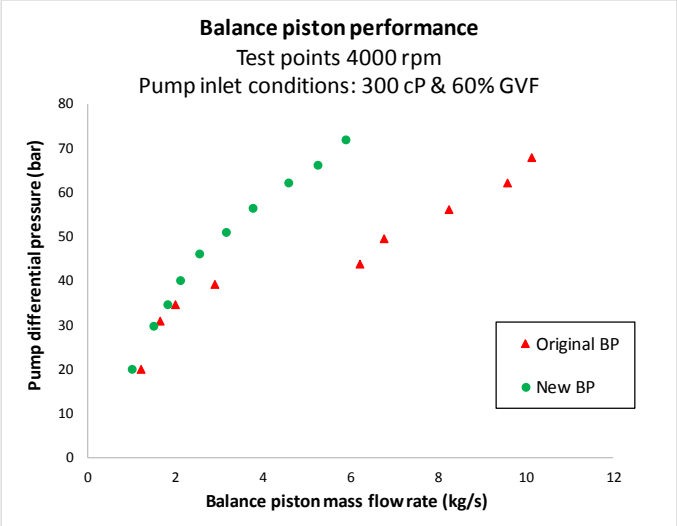

Figure 23 Balance piston leak rates – original and new balance piston

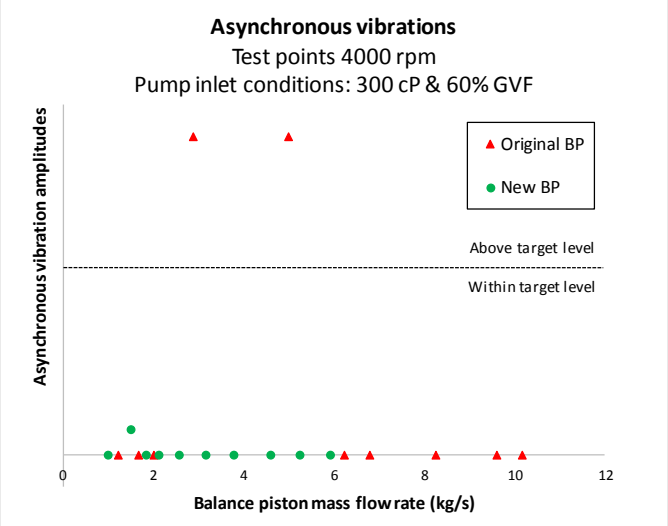

Figure 24 Asynchronous vibrations – original and new balance piston

SUMMARY AND CONCLUSIONS

Annular seals subjected to multiphase viscous flow with axial pressure gradient are applied as balance pistons and seals in HighBoost multiphase boosting pumps for oil and gas. The pumps are usually located subsea with limited intervention possibilities, and with no upstream processing or treatment of the well stream. The boosting pumps hence need to be highly flexible in terms of operating conditions, and utterly robust.

Although dynamics in annular seals is a popular research topic, the available research on multiphase viscous flow in annular seals is very limited. Several correlations for two-phase mixture viscosity exist, with results yielding differences of several orders-of-magnitude. Calculated leak rates, temperatures and rotordynamic seal coefficients based on mixture viscosities are therefore highly uncertain.

During a range-extending full-scale pump test, the authors discovered a phenomenon creating a major step change in balance piston throughflow along with significant rotor vibrations. The phenomenon manifested itself as transitional, occurring only at intermediate viscosities, intermediate GVFs, and intermediate differential pressures. The authors did not succeed in reproducing the transitional behavior with existing analytical models. However, multiphase CFD simulations gave valuable results, both in visualizing flow structures and generating rotordynamic seal coefficients.

By extensive full-scale testing and analysis, the authors have succeeded in developing a high-viscosity MPP balance piston which mitigates the negative effects of flow transition and allows for pump operation at differential pressures up to at least 1,595 psi (110 bar), liquid viscosities between 1 and 800 cP (0.001-0.8 Pa·s), and unlimited GVFs. The pump is installed subsea at the Moho field off the coast of the Republic of the Congo, where it is boosting unprocessed well flow consisting of viscous oil, water, and gas.

Further work

Although the pump manufacturer succeeded with their goal on developing a multiphase pump with balance piston allowing stable operation at the desired span in flow regimes, fluid models describing the transition onset and dynamic effects are continuously being improved. CFD is undoubtfully an extremely valuable tool with its possibilities of providing a qualitative, visual view of the flow structures along with quantitative determination of frictional losses and fluid dynamic forces. Experiments are currently being performed for optimization and validation of CFD models. Additional theoretical and experimental investigation of fluid forces in a High-Viscosity HighBoost shaft-bearing system is ongoing.

NOMENCLATURE

BP	= Balance Piston	
C	= Gap clearance	(m)
CFD	= Computational Fluid Dynamics	
DE	= Drive End	
dP	= Differential Pressure	(psi) or (bar)
EPC	= Engineering, Procurement and Construction	
GVF	= Gas Volume Fraction	(-)
JIP	= Joint Industry Project	
K	= Stiffness	(-)
L	= Seal length	(m)
LAS	= Liquid Annular Seal	
L/D	= Length Diameter ratio	(-)
NDE	= Non-Drive End	
MPP	= Multiphase Pump	
Q	= Volumetric flowrate at P,T	(gpm) or (m^3/h)
R	= Radius	(m)
Re	= Reynolds number	(-)
Ro	= Rossby number	(-)
Ta	= Taylor number	(-)
u	= Velocity	(m/s)
VSD	= Variable Speed Drive	
μ	= Viscosity	(cP) or (Pa·s)
ρ	= Density	(kg/m^3)
Φ	= Two-phase multiplier	(-)
ω	= Angular velocity	(rad/s)

Subscripts

ax	= axial
g	= gas phase
i	= inner
l	= liquid phase
leak	= leakage across balance piston
m	= mixture
r	= radial

tan = tangential
xx = direct
xy = cross-coupled

REFERENCES

Arauz, G. L., San Andrés, L., 1998. Analysis of Two-Phase Flow in Cryogentic Damper Seals – Part 1: Theoretical Model. J Tribol., 120(2), 221-227.

Beattie, D. R. H., Whalley, P. B., 1982. A Simple Two-Phase Flow Frictional Pressure Drop Calculation Method. Int. J. Multiphase Flow, 8: 83-87.

Beatty, P. A., Hughes, W. F., 1990. Stratified Two-Phase Flow in Annular Seals. J Tribol., 112(2), 372-381

Bibet, P. J., Lumpkin, V. A, Klepsvik, K. H., Grimstad, H. J., 2013. Design and Verification Testing of New Balance Piston for High Boost Multiphase Pumps. The Twenty-Ninth International Pump Users Symposium

Black, H. F., Jenssen, D. N., 1970. Dynamic Hybrid Bearing Characteristics of Annular Controlled Leakage Seals. Proc Instn Mech Engrs, Vol. 184, 92-100.

Childs, D. W., 1983. Dynamic Analysis of Turbulent Annular Seals Based on Hirs' Lubrication Equation. ASME Journal of Lubrication Technology, Vol. 105, 429-436

Childs, D. W., Rodrigues, L. E., Cullotta, V., Al-Ghasem, A., Graviss, M., 2006. Rotordynamic-Coefficients and Static (Equilibrium Loci and Leakage) Characteristics for Short, Laminar-Flow Annular Seals. J Tribol., 128(2), 378-387.

Dukler, A. E., Wicks, M., Cleveland, R. G., 1964. Frictional Pressure Drop Two-Phase Flow. AIChE J, 10: 38-51.

Iwatsubo, T., Nishino, T., 1994. An experimental study on the static and dynamic characteristics of pump annular seals with two phase flow. NASA. Lewis Research Center, Rotordynamic Instability Problems in High-Performance Turbomachinery, 1993; 49-64.

McAdams, W. H., Woods, W. K., Heroman, L. C., 1942. Vaporization inside horizontal tubes-II. Benzene-Oil Mixtures. Trans. ASME, 64: 193.

San Andres, L., 2012. Rotordynamic Force Coefficients in Bubbly Mixture Annular Pressure Seals. ASME J. Eng. for Gas Turbines Power, Vol. 134, 022503.

San Andres, L., Lu, x., Liu, Q., 2016. Measurements of Flow Rate and Force Coefficients in a Short-Length Annular Seal Supplied with a Liquid/Gas Mixture (Stationary Journal). Tribology Transactions, 59:4, 758-767.

Shiomi, Y., Kutsuna, H., Akagawa, K., Ozawa, M., 1993. Two-Phase Flow in an Annulus with a Rotating Inner Cylinder (Flow Pattern in Bubbly Flow Region). Nuclear Engineering and Design 141: 27-34.

Storteig, E., 1999. Dynamic Characteristics and Leakage Performance if Liquid Annular Seals in Centrifugal Pumps. Ph. D. Thesis, Norwegian University of Science and Technology.

Tran, Dung L., 2018. Experimental Study of the Static and Dynamic Characteristics of a Long (L/D=0.75) Smooth Annular Seal Operating under Two-Phase (Liquid/Gas) Conditions with Three Inlet Preswirl Configurations. M.Sc. Thesis, Texas A&M University.

Vannini, G., Masala, A., Neri, M. O., Evangelisti, S., Camatti, M., Svetti, F., Bondi, S., 2011. Full Load Testing of a 12.5MW Vertical High Speed Subsea MotorCompressor. The Fortieth Turbomachinery Symposium.

Werely, S. T., Lueptow, R. M., 1999. Velocity Field for Taylor -Couette Flow with an Axial Flow. Physics of Fluids, 11, 3637-3649

Yamada, Y., 1962. Resistance of a Flow through an Annulus with an Inner Rotating Cylinder. Bulletin of JSME, Vol. 5, No. 18, 302-310

ACKNOWLEDGMENTS

The authors thank the project team for the efforts and collaboration during this project. A special thank you also to the Companies for the permission to publish this information and contribute to the knowledge sharing in the rotordynamics technical community.